DAVID M. RUST, JOHN W. O'BYRNE, and TERRY J. HARRIS

AN OPTICAL INSTRUMENT FOR MEASURING SOLAR MAGNETISM

A new instrument for measuring solar magnetic fields, the solar vector magnetograph, is under construction at APL's Center for Applied Solar Physics. Its key attributes are high spatial resolution, high optical throughput, fine spectral selectivity, and ultra-low instrumental polarization. A 25-cm Cassegrain telescope will provide 0.7″ angular resolution. Spectral selection will be accomplished with an electrically tunable solid Fabry–Perot filter with a bandwidth of 0.0175 nm. The polarization analyzer should achieve a sensitivity of 1:4000. When assembled, the instrument will be tested at APL and then moved to the National Solar Observatory in New Mexico, where it will operate during the upcoming period of peak activity (1989–93).

INTRODUCTION

The sun is a perfect sphere—a flawless, brilliant yellow orb, seemingly all quietude and beneficence—until a view through a telescope reveals its boiling surface and the famous sunspots. Above the sunspots the temperature rises abruptly from 6000°C to 2,000,000°C. In that sensitive transition region, magnetic fields from the sunspots spread out and twist the solar gases into fantastic shapes (Fig. 1). The dynamics of those solar prominences are apparent in movies made with telescopes that suppress light from the brilliant photosphere below. Occasionally, the films reveal sudden brightenings (called flares)[1] and ejections of material (called sprays). Those events have a profound impact on man's activities in space and on the upper atmosphere of Earth (Fig. 2).

At present, flares are unpredictable, but we believe that research into the structure and evolution of the magnetic fields from which they draw their energy will eventually allow them to be understood and forecast. Such a level of understanding is the principal objective of APL's Center for Applied Solar Physics, which is now in the second year of an interdisciplinary program of optical instrumentation development and fundamental research on solar magnetic fields.

SCIENTIFIC BACKGROUND

Solar flares and their effects on earth are unpredictable because we do not yet know how to extract enough information from preflare observations. What we do know is that solar flares occur in so-called active regions that are composed of intertwined magnetic flux tubes.[2] Magnetic flux emergence and thermal convection cause active regions to evolve toward increasing complexity and to produce highly sheared and stressed tangles of magnetic fields. Major changes occur in less than an hour. The sheared fields are reservoirs of stored magnetic energy (approximately 10^{25} J) that can be liberated via explosive instabilities, especially if there is a triggering perturbation.[3,4]

The emergence of fresh magnetic flux in existing active regions clearly triggers flares when a marginally stable configuration exists[3] (Fig. 3). Then an eruption results that blows open the magnetic arcades above the active region. Reconnection of the disrupted fields causes intense heating (to 100,000,000°C) and the emission of X rays that affect radio-wave propagation in Earth's ionosphere. In addition, a shock wave explodes into interplanetary space, and, depending on the magnetic fields it encounters, it may strike Earth 1 to 3 days later.

Progress in forecasting individual flares, as opposed to issuing warnings based on statistics, is still in an embryonic phase. The most promising signal of an imminent major flare appears to be emerging magnetic flux in the photosphere. Early detection of emerging magnetic fields, which may be only a few tens of millitesla in strength, might give several hours of warning before a major flare onset. That indicator is not now used in any systematic forecasting scheme, largely because the necessary observations (which require very sensitive magnetographs) are not routinely available. We hope a magnetograph such as the one now under development will eventually be stationed in space to monitor constantly for the magnetic field changes that presage solar flares.

The goal for the Center for Applied Solar Physics vector magnetograph is to measure all three components of the magnetic field with a sensitivity of 0.005 to 0.01 T and a spatial resolution on the sun of 500 km (Fig. 4). Such specifications are beyond the reach of present instruments, most of which were built 20 or more years ago. Using modern optical devices, such as ultra-narrowband filters, liquid-crystal and laser-quality polarization analyzers, and a solid-state camera based on charge-coupled-device (CCD) technology, we are assembling a magnetograph that should meet the scientific performance goal. It will be placed first at the Sacramento Peak Observatory, at Sunspot, N. Mex. (near Alamogordo), where it can take advantage of the clear skies and excellent image quality. Later, we hope to carry the instrument to

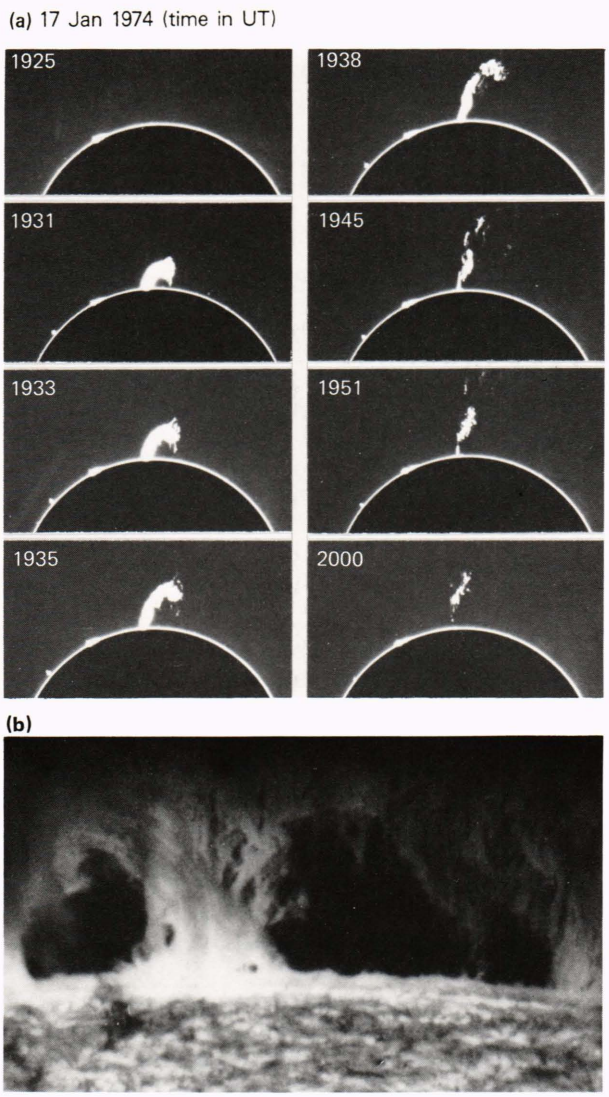

Figure 1—(a) Development of a "spray" from the sun. The bright solar disk itself, called the photosphere, has been occulted by a black disk so that the fainter spray can be recorded. Note that the height of the spray is comparable to the solar radius (700,000 km). (b) Close-up view of a solar prominence. Such structures frequently become unstable and erupt, as shown in Fig. 1a. The prominence rises to a height of approximately 50,000 km above the solar surface.

30-km altitudes with a balloon, in order to be completely free of the image degradation caused by turbulence in our atmosphere.

MEASUREMENT PRINCIPLE

The intensity and direction of the magnetic field at the solar surface may be inferred from measurements of the polarization of sunlight in very narrow spectral bands. That effect was discovered in the laboratory by P. Zeeman in 1896, and it was applied very shortly thereafter by G. E. Hale to the measurement of magnetic fields in sunspots.[5]

The Zeeman effect is characterized by the splitting of atomic spectral lines into two or more orthogonally polarized components, which occurs when the atoms emitting the light are in a magnetic field (Fig. 5). If the field direction is strictly parallel with the line of sight to the viewer, the split components will be circularly polarized; if the field is perpendicular to the line of sight, the atomic emissions will consist of a linearly polarized component with no shift from the atomic reference wavelength and two or more other components at longer and shorter wavelengths with linear polarization orthogonal to that of the unshifted component. The relative strength of the various components as a function of wavelength is measured by a vector magnetograph and is expressed in terms of the four Stokes parameters I, Q, U, and V.[6] The magnetic field may be inferred from those parameters using the theory of the formation of spectral lines in a stellar atmosphere.[7]

To achieve the desired sensitivity in all components of the vector field, it is necessary to measure polarization with a sensitivity of 1 part in 4000 (Fig. 6). How this can be accomplished will be discussed after a review of the vector magnetograph optical layout.

SOLAR VECTOR MAGNETOGRAPH DESIGN

The new technologies for detectors, filters, and polarization modulators that have become available recently are important for the realization of significant improvement in vector magnetograph results. Included in the vector magnetograph optical path are a waveplate/polarizer for polarization analysis, a narrow-band bandpass blocking filter, and an image motion compensator to counter atmospheric turbulence effects. Shown in Fig. 7, the optical layout consists of a reflecting telescope with a 25-cm aperture and a series of mostly off-the-shelf lenses that control the solar beam diameter through the instrument and ultimately focus an image of a portion of the sun onto a CCD detector array.

Because the vector magnetograph must be mounted on an existing spar (Fig. 8) at the Sacramento Peak Observatory, its size must be less than 3 m $\times$ 0.5 m and its weight less than 180 kg. After installation of the vector magnetograph, the spar must be carefully balanced so that it can point to within 1″ of the center of the sun throughout the day. For this reason, the center of gravity must be precisely known. The same considerations will apply to a balloon-borne vector magnetograph.

The observatory is located at an altitude of 2800 m above sea level, which can make for a fairly severe thermal environment. In winter, temperatures can fall below -18°C and summer temperatures can reach 32°C. On many days, the temperature changes by more than 6°C/h. Therefore, active thermal and mechanical controls are required to stabilize focus and alignment and to prevent passband shifts and other temperature-dependent changes in sensitive optical and electronic components. The structure supporting the magnetograph optics must be very rigid because the relative gravity vector varies as the spar follows the sun across the sky. Flexure in the mechanical housing must not shift the image on the detector by more than 0.25 pixel during a mea-

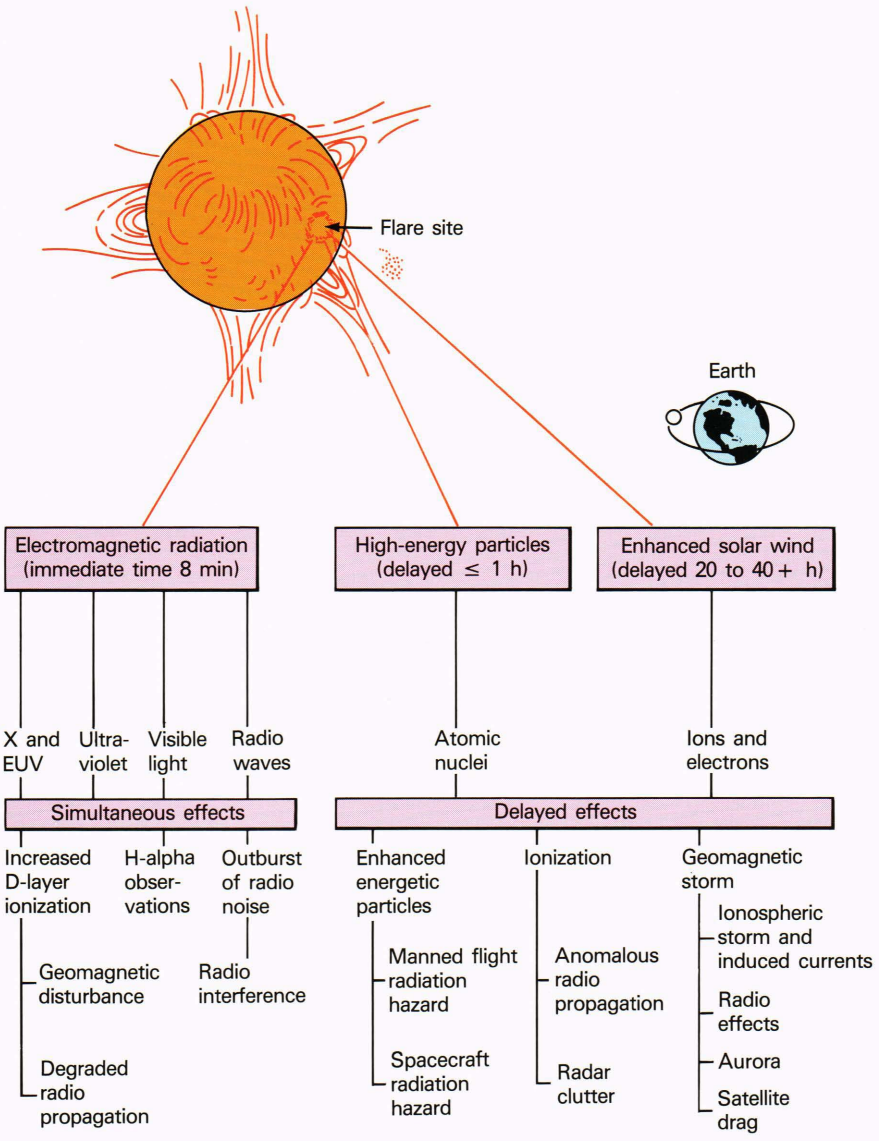

Figure 2—The effects of solar flares on earth.

surement sequence. Additionally, the observer will not necessarily want to point the telescope at sun center, so two mounts are required: a gimbal mount and a mount with two translation axes. Thus, the stiffness inherent in the spar will be of little assistance in fighting misalignment.

ULTRA-NARROW OPTICAL BANDPASS FILTER

Spectral discrimination is accomplished with a large-aperture, tunable, solid Fabry–Perot etalon.[8] Solid Fabry–Perot etalons are lightweight and rugged, but, until recently, they could not be tuned. As a result of a successful development program in cooperation with the Division of Applied Physics of the Australian Commonwealth Scientific and Industrial Research Organization, a 75-mm- diameter tunable filter with excellent flatness is available (Fig. 9). Its passband is 0.0175 nm and its free spectral range (the spacing between successive passbands) is 0.35 nm.

In a Fabry–Perot etalon, the higher the refractive index of the spacer, the less the passband shifts and broadens for off-axis rays. The wavelength shift is given by

$$\Delta\lambda/\lambda = \phi^2/2n^2 \ , \qquad (1)$$

where ϕ is the angle between the incoming ray and the normal to the filter and n is the index of refraction of the spacer. Thus, the acceptance cone of the lithium-niobate etalon, for which $n = 2.3$, is 5 times that of an air-spaced etalon. In other words, for the same spatial and spectral resolution, an air-spaced etalon must have 5 times the area of a lithium-niobate etalon, when used in an instrument with the same total field of view and telescope aperture.

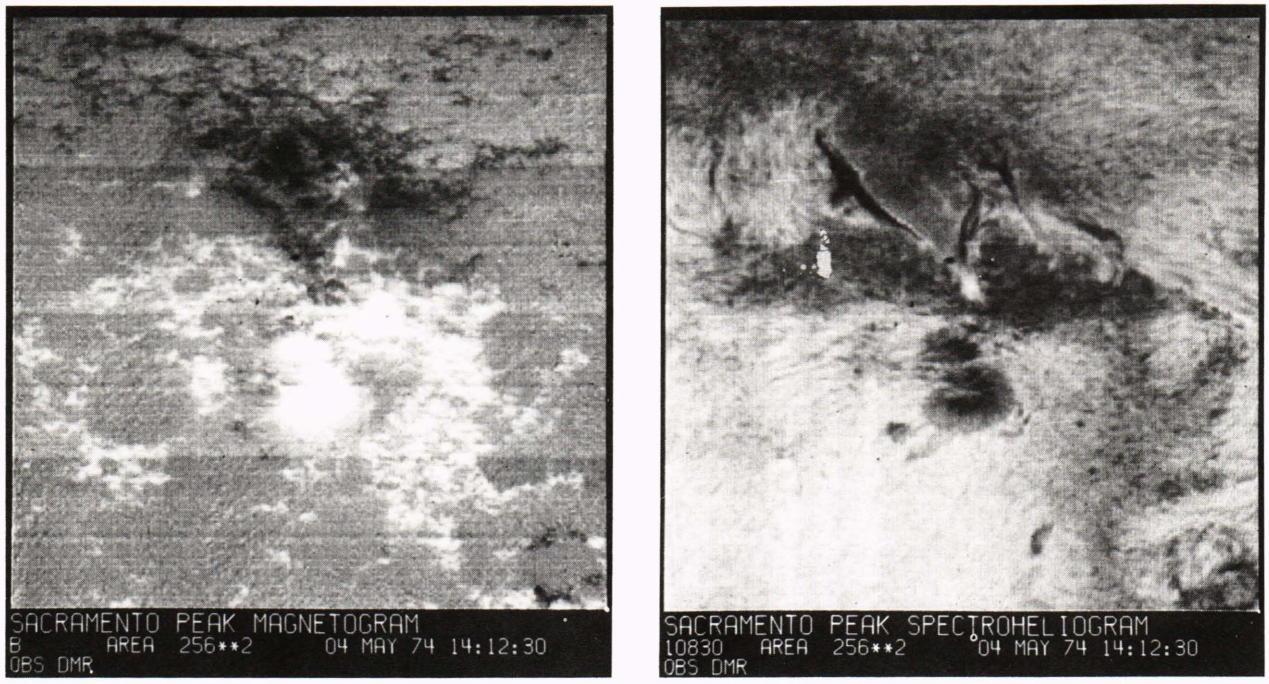

Figure 3—A map of the line-of-sight magnetic fields (left) and of the helium emission (right) in a solar active region. In the magnetogram, white areas denote outward-directed fields, and black areas denote inward-directed fields. Visible in the helium picture are sunspots, filaments (which are prominences seen in projection above the solar disk), and a small solar flare (the bright area just above the sunspots).

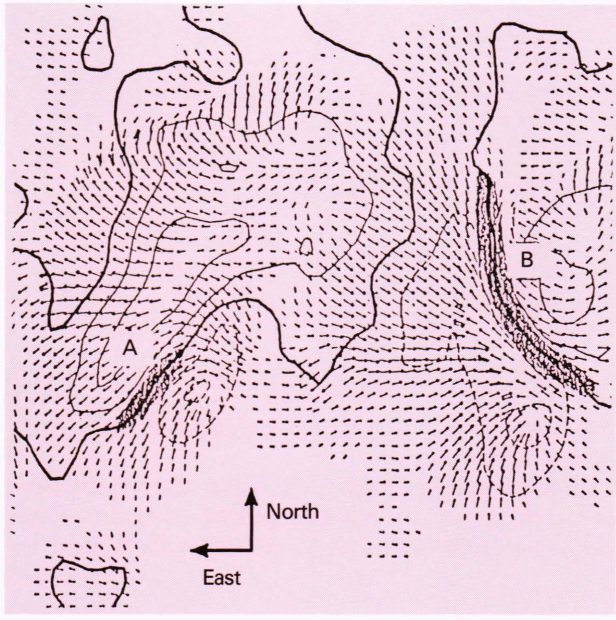

Figure 4—A map of the magnetic field vectors in a solar active region (map supplied by NASA Marshall Space Flight Center, 1984). The length of each arrow is roughly proportional to the strength of the transverse magnetic field, but the absolute calibration is uncertain.

Mechanical means are usually used to tune Fabry–Perot filters, either by varying the spacing between the mirrors (for air-spaced filters) or by tilting with respect to the beam. In lithium niobate, application of an electric field along the optic axis induces a change in the refractive index of

$$\delta n = -\tfrac{1}{2}\, n_0^3\, r_{13}\, E_3 \qquad (2)$$

for light propagating along the optic axis, where n_0 is the refractive index in the absence of a field, r_{13} is the relevant linear electro-optic coefficient, and E_3 is the applied field. The passband can be shifted to any wavelength within its free spectral range by application of $\pm\tfrac{1}{2}\, V_{1/2}$, where

$$V_{1/2} = \pm \frac{\lambda}{n_0^3\, r_{13}}\ , \qquad (3)$$

where λ is the wavelength of the light.

For $\lambda = 610$ nm, the theoretical value of $V_{1/2}$ is 5500 V, but because of the piezoelectric effects in the lithium niobate crystal, $V_{1/2} \approx 8700$ V. Fortunately, the tuning requirements of a solar magnetograph are modest. Only temperature drifts in the instrument and Doppler shifts caused by Earth's orbital motion must be compensated for and both are less than 0.02 nm. Thus, ± 500 V will provide adequate control over the passband. Voltages up to one-half of $V_{1/2}$ would be needed in a more versatile instrument, one that can be used in conjunction with several narrow-band order-isolation filters to study many spectral lines.

Last year, we conducted an extensive series of tests of Fabry–Perot filter elements. We tested the filter's ability to withstand voltage cycling equivalent to 10 years' oper-

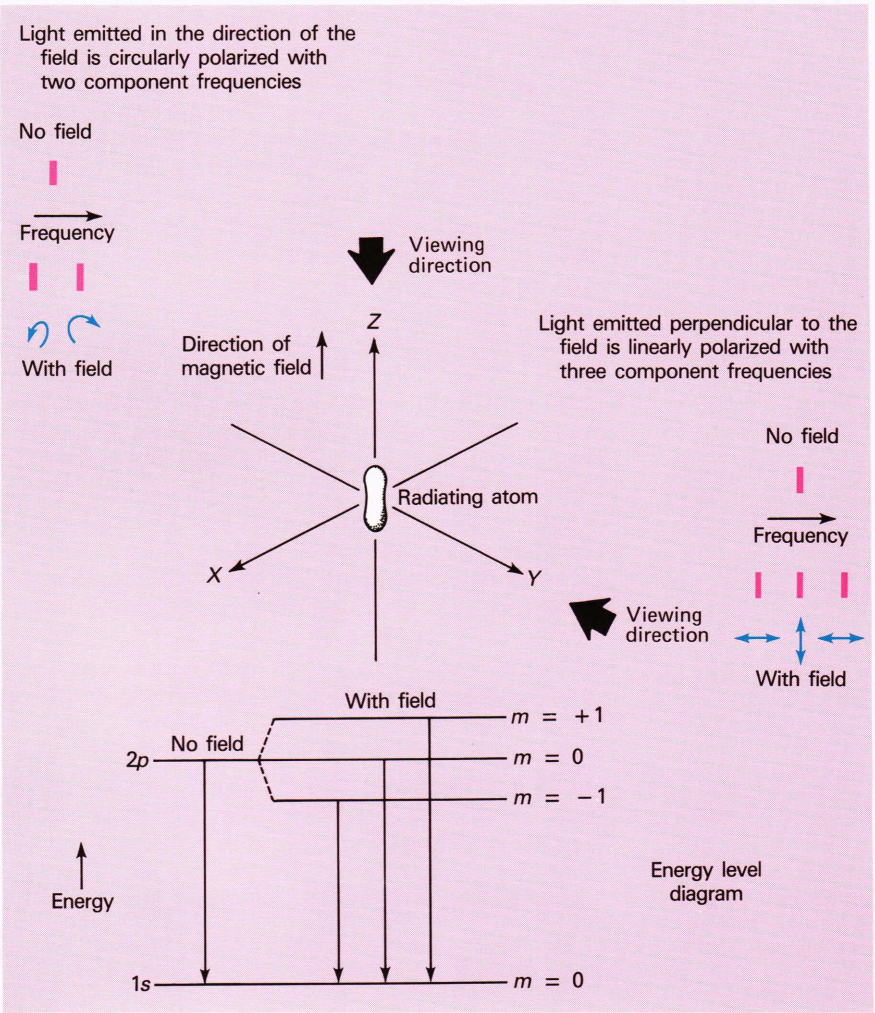

Figure 5—The effect of a magnetic field on the polarization and spectrum of light emitted by an atom.

ation and to survive bombardment by 70-MeV protons, a level similar to that of the energetic flare-generated protons in space. No deterioration was found. Similarly, the filter withstood the vibration of a simulated shuttle launch.

MAINTAINING HIGH THROUGHPUT AND IMAGE QUALITY IN THE VECTOR MAGNETOGRAPH

Use of Fabry–Perot filters and a commercial polarizer requires special attention to beam diameters in the magnetograph. The beam diameter at the filter should be large to minimize the cone angle, because the passband broadens in proportion to the square of that angle. A large but different beam diameter must be used at the blocking filter for similar reasons, while the small aperture of the available prism polarizer dictates a narrow beam at that point. To avoid spherical aberration (and the use of expensive custom optics to correct for it), the beam through each of these components is collimated. Also, the optical elements in front of the polarization analyzer must be circularly symmetrical to minimize instrumental polarization.

The objective telescope for the vector magnetograph is a 25-cm-aperture Cassegrain telescope. At the design wavelength of 610.4 nm, the telescope resolution is limited by diffraction to 0.62″. The internal image plane of the telescope is water-cooled, and the entire telescope assembly is evacuated to eliminate local air turbulence caused by the high temperatures at the internal focused solar image. To avoid aliasing or loss of resolution at the detector, the image scale is set so that 0.25″ in the field corresponds to one detector element. Since there are 384 × 576 elements, the instrument field of view is 1.6′ × 2.4′. The field may be doubled at the cost of a factor of 2 in resolution. The larger field will encompass all but the largest solar active regions.

The telescope is followed in the optical path by a field lens that forms an image of the telescope aperture at the image-motion-compensator mirror, whose function is described below. A second lens collimates the beam and passes it through an infrared rejection filter to the polarization analyzer. The field lens located near the telescope external focus helps to control the beam diameter through the polarimeter section so that it is transmitted without vignetting. The beam diameter through the

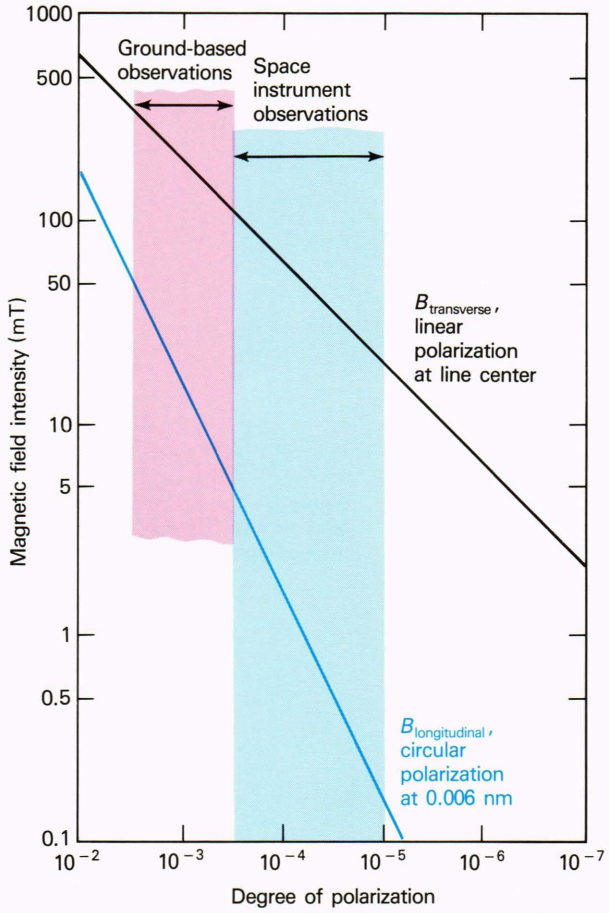

Figure 6—The longitudinal and transverse magnetic field strength in the photosphere that may be inferred from the indicated degree of circular and linear polarization.

polarimeter is 17 mm with a maximum off-axis angle of 0.6°.

Following the beam-splitter in the main optical path are two positive achromatic cemented doublet lenses that expand the collimated 17-mm beam to 43 mm to fill the clear aperture of the blocking filter. A second beam expander of Galilean design (with one positive element and one negative element) expands the 43-mm beam to 69 mm through the Fabry–Perot filter. The combined powers of the beam-expander elements locate a pupil image at the Fabry–Perot filter. Thus, imperfections in the Fabry–Perot filter will affect all points in the solar image equally. The maximum angle for rays entering the Fabry–Perot filter is 9′, which corresponds to a maximum spectral shift over the field of view of less than 4×10^{-4} nm.

Both the Fabry–Perot filter and the thin-film blocking filter are maintained in temperature-controlled housings to stabilize their passbands. Both filters may be tuned by means of computer-controlled actuators that can tilt each filter axis relative to the optical axis. High-voltage leads are connected to the Fabry–Perot filter for rapid passband tuning. After the Fabry–Perot filter, a custom-designed air-spaced achromatic doublet lens is combined with a flat-field 10× microscope objective to focus the final solar image onto the CCD. Such an arrangement takes advantage of the magnifying power of well-corrected off-the-shelf microscope optics to reduce the overall system length. The doublet lens, which is a critical element in obtaining the necessary spatial resolution in the magnetograph, is relatively fast (f/6.8), and it gives good correction of chromatic and geometric aberrations in the red portion of the spectrum. A 5× microscope objective can be used with the achromat to double the field of view at the expense of resolution.

IMAGE MOTION COMPENSATOR

The sequences of exposures required to build up low-noise magnetograms will be 1 to 20 min long. Thus, the solar image in the CCD camera must be held stable, which is the job of the image motion compensator (IMC). The IMC beam-splitter transmits a small percentage of the sunlight into the system, while directing most

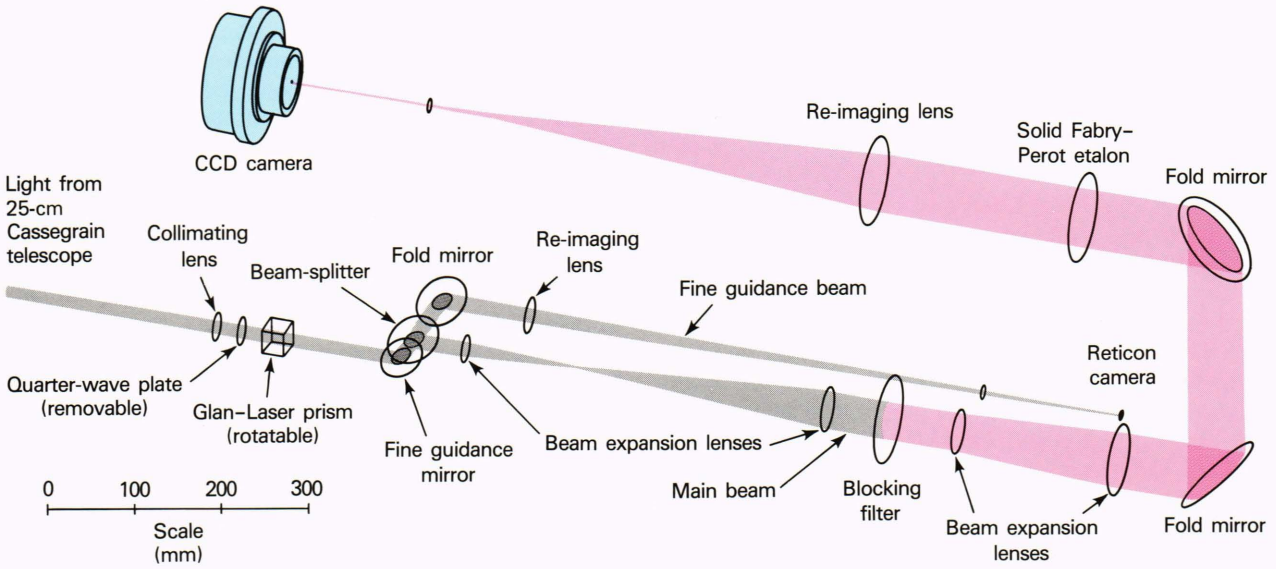

Figure 7—Optical layout of the vector magnetograph.

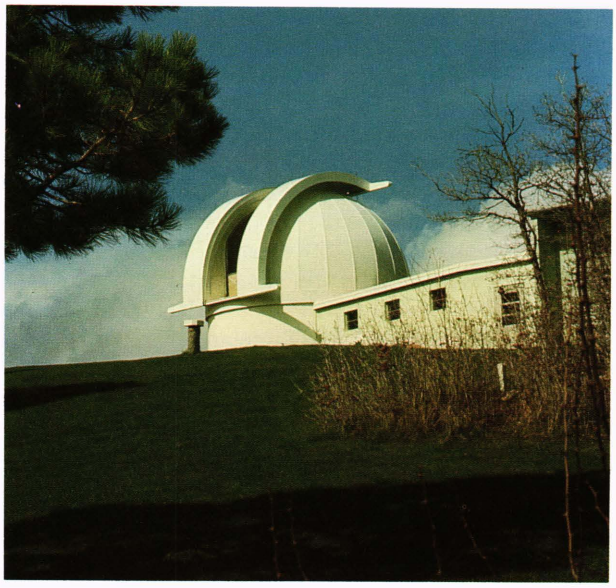

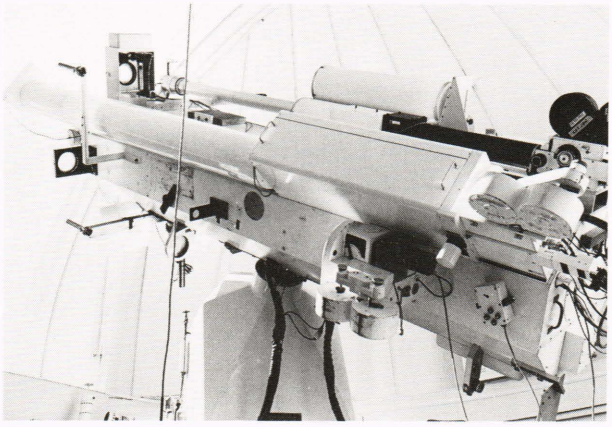

Figure 8—(top) The vector magnetograph will be mounted inside the Sacramento Peak Observatory in the Sacramento mountains in Sunspot, N. Mex. (in the southern part of the state). (bottom) A cluster of solar telescopes on the faces of the octagonal spar at the Sacramento Peak Observatory. The vector magnetograph will replace the components attached to the face closest to the viewer.

of the light into the main optical path. The IMC optics consists of an achromatic 500-mm focal length lens and 10× flat-field microscope objective, which focus an image of the sun onto a 32 × 32-element photodiode array. The images from the photodiode array are analyzed to produce signals to the three piezoelectric stacks that steer the IMC mirror to remove transverse motion at the final image plane.

The heart of the IMC is a sequential binary correlation (SBC) algorithm for computing the solar image offset from a reference image. The IMC mirror position is updated at a 50-Hz rate as the sensed image is compared with the periodically updated reference image. The images cover a sector of only 10″ × 10″, but they need not contain high-contrast features for the algorithm to operate effectively.

Kim Strohbehn and Patricia Murphy at APL have tested the SBC algorithm using solar granulation data

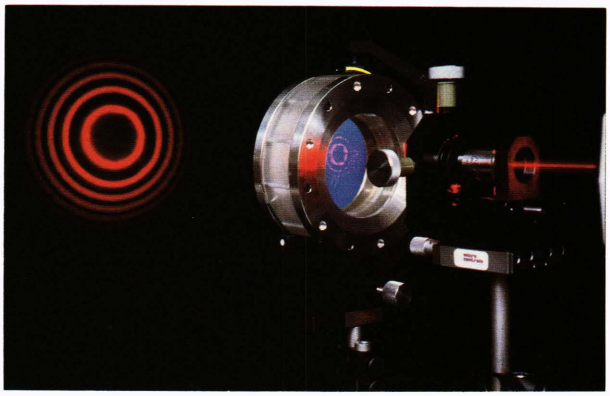

Figure 9—Photograph of the Fabry-Perot etalon illuminated by a divergent laser beam. The classic Fabry-Perot ring pattern illustrates the varying response of the filter with the angle of the incident beam of light. The lithium-niobate etalon is manufactured by CSIRO Division of Applied Physics, Sydney, Australia.

obtained by R. B. Dunn at the Sacramento Peak Observatory. Their tests show that a fast, binary registration gives nearly the same results as conventional, slower, gray-scale registration. The SBC algorithm introduces rms pointing errors of approximately 0.02″, which is negligible relative to the 0.25″ pixels of the CCD. Strohbehn has implemented the SBC algorithm in custom hardware for the vector magnetograph.

POLARIZATION ANALYZER

The polarization analyzer passes various combinations of linear and circular polarization, according to a programmed sequence. Any variation in the transmitted beam can be related to the polarization state of the sunlight. It is important that this polarization analyzer produce minimum cross talk between the circularly polarized signal and the generally weaker linear signal. Cross talk is caused by unavoidable imperfections in the retardation, extinction, or positioning of the polarizing elements. A study at NASA's Marshall Space Flight Center[9] suggests that a removable quarter-wave retarder followed by a rotating-prism polarizer will minimize cross talk. The prism alone is used to measure linear polarization states, and the retarder is introduced only in measurements of the circular state.

The polarizing prism turns in a computerized rotary stage that achieves 3.6″ resolution and reproducibility of prism orientation. The quarter-wave plate is translated in and out of the beam, but it retains a fixed orientation when in the beam. This minimizes the positioning errors that can introduce cross talk. The retarder is not in the beam for the linear measurements and cannot be a source of cross talk from the circular signal to the linear signal. The usual approach of rotating the quarter-wave plate was avoided, because rotation may introduce spurious modulation in the transmitted beam (reflection at waveplate surfaces depends on the orientation of the crystal axes relative to the polarization of the incident beam).

The quarter-wave plate consists of several layers of birefringent polymer materials cemented between opti-

cally polished windows. It functions by retarding light that is polarized parallel to one of its two optical axes. The retardation is 0.25 λ at 610 nm and is constant to better than 4% over a 200-nm band. Therefore, we expect the retarder to have excellent temperature stability within the vector magnetograph's operating band of approximately 0.05 nm. It has good optical quality (λ/10 surface flatness) and is specially chosen to introduce less than 10″ beam deviation.

The polarizing prism is a Glan–Laser prism, which is a form of air-spaced Glan–Taylor prism modified for the high power requirements of laser use. The most obvious special feature is an exit port provided in the mounting cylinder to allow light of the unwanted polarization to escape. This type of prism was chosen in part because of the possibility of high power levels in a solar instrument.

The major advantages of the Glan–Taylor prism are its very high transmission and very good extinction ratio of less than 5×10^{-5} (that is, the ratio of the transmitted light polarized parallel to one axis to that of the other polarization). The Glan–Laser prism has the disadvantage of a very small acceptance half-angle (1.25°). Light that is farther off-axis than this may be rejected or not polarized by the prism. When the vector magnetograph field of view is considered, this implies that the prism must be aligned to better than 0.5°. Also, the prism introduces a beam deviation of 1′ 50″, which, if uncorrected, would produce a significant field shift on the image plane as the prism rotates. Two small-angle wedges were positioned behind the prism to reduce the beam deviation.

To obtain the highest possible polarimetric accuracy, a dichroic polarizer will augment the Glan–Laser prism. Ours consists of an HN38 Polaroid polarizer cemented between good-quality optical windows. The combination of prism and dichroic achieves an extinction ratio of approximately 10^{-8} while retaining good optical quality and relatively high transmission.

A quarter-wave plate is also attached to the rear of the polarizing assembly. The fast axis of the wave plate is oriented at 45° to the transmission axis of the polarizers; it circularly polarizes the light. The output beam is then insensitive to subsequent elements, such as fold mirrors, which themselves act like linear polarization analyzers. If this step were not taken, the transmitted intensity would be modulated by the following optics as the prism rotates.

The entire polarizing assembly can be removed from the optical train for test or modification. It may even be replaced someday by a liquid-crystal polarization rotator (one such device is under study now). It simulates a half-wave plate whose orientation may be varied through 45° by the application of ±15 V. In their ability to modulate plane-polarized light, liquid-crystal devices are remarkably insensitive to pressure, temperature, and minor voltage errors.

POLARIZATION ANALYSIS

Most atomic spectral lines are affected by the presence of a magnetic field (Fig. 5). Because of variations in atomic structure, some lines are more sensitive than others, and they are more suitable for analysis with the vector magnetograph. Derivation of the vector magnetic field requires polarization measurements at various points across a magnetically sensitive spectral line. At each wavelength, the polarization state of the incident light is conventionally expressed[8] in terms of the Stokes parameters I, Q, U, and V. Here I is the total light intensity, Q represents the "preference" for light linearly polarized at (say) 0°, U represents the preference for linear polarization at 45°, and V (as used below) represents the preference for left-hand circular polarization.

The following irradiance measurements can be made, assuming the quarter-wave plate has its fast axis aligned with the 0° prism angle; each irradiance is expressed in terms of the equivalent combination of Stokes parameters:

Prism Angle (deg)	*Wave Plate Out*	*Wave Plate In*
0	$I + Q$	$I + Q$
45	$I + U$	$I + V$
90	$I - Q$	$I - Q$
135	$I - U$	$I - V$

Measurements for prism angles from 180° to 360° simply repeat and are useful for calibration purposes.

Six measurements can be used to derive the Stokes values:

$$S_{q1} = I + Q ,$$
$$S_{q2} = I - Q ,$$

then

$$Q/I = (S_{q1} - S_{q2})/(S_{q1} + S_{q2}) ;$$

$$S_{u1} = I + U ,$$
$$S_{u2} = I - U ,$$

then

$$U/I = (S_{u1} - S_{u2})/(S_{u1} + S_{u2}) ;$$

$$S_{v1} = I + V ,$$
$$S_{v2} = I - V ,$$

then

$$V/I = (S_{v1} - S_{v2})/(S_{v1} + S_{v2}) .$$

The intensity I can be determined as $I = \frac{1}{2}(S_{q1} + S_{q2})$, and similarly for the U and V components. Thus, in principle, only four of the above measurements are required—say, S_{q1}, S_{q2}, S_{u1}, and S_{v1}. In practice, S_{v2} may also be measured to provide an independent measure of I when using circular polarization.

Individual measurements of each state do not provide sufficient signal-to-noise ratio to obtain the desired polarimetric accuracy. It is therefore necessary to add many frames together to obtain the desired signal-to-noise ratio. System throughput calculations for the vector mag-

netograph predict a photoelectron generation rate of approximately 3×10^6 electrons/s per 0.5″ pixel on the CCD. Thus, 75% of saturation of the CCD is expected to be reached in approximately 0.13 s. Neglecting the effect of intensity fluctuations induced by atmospheric turbulence, shot-noise statistics indicate that 48 frames will be required to reach the 1:4000 accuracy desired for the linear components. Suitable accuracy for the circular component can be achieved with only 12 frames, because the signal is so much stronger for a given magnetic field.

Since actual exposure times are short, the CCD readout and frame storage rates determine the total measurement time. If we assume approximately 2 s processing time per frame, then approximately 18 min are required for the polarization measurements at three wavelengths. Somewhat shorter intervals than this are best for studying the temporal variation of the magnetic field, so more rapid methods of reading the CCD and handling the data are being sought. Calculation and display of the vector magnetic field may be performed during the interval between observing sequences.

DETECTION SYSTEM

The vector magnetograph detector uses a commercial solid-state camera with a 384 × 576 CCD array of 23-μm-square pixels, each with a capacity (well depth) of 500,000 photoelectrons. To reduce thermal electron noise in the detector to negligible levels, a thermoelectric cooler holds the array at $-50°$C.

The CCD housing has an electronically controlled mechanical shutter. Minimum exposure time is 0.2 s, although the corresponding time for the camera to complete all acquisition activities with 12-bit accuracy is at least 1 s.

The camera head is driven from a nearby electronics unit, which in turn is controlled by a single-board computer based on a 68020 microprocessor. Image data may be displayed on a monochrome video display or a color monitor that has an associated color hard-copy unit. Data are stored on a 720-kB floppy disk drive, a 140-MB Winchester disk drive, a 40-MB ¼-in. cartridge tape drive, and a 9-track tape drive. Twelve serial ports are provided for interfacing to external devices.

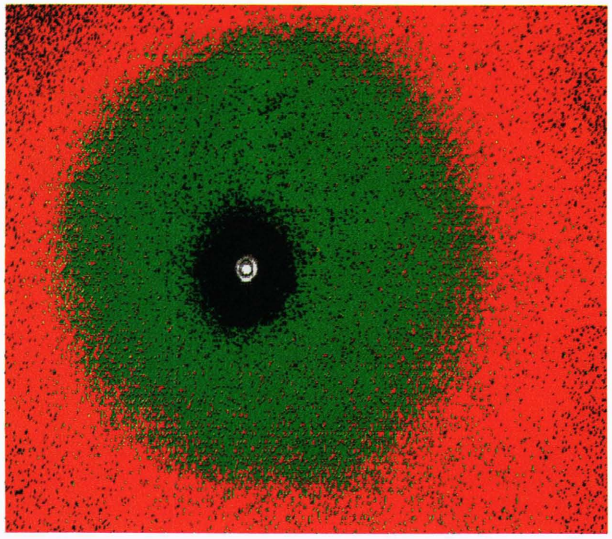

Figure 10—Vector magnetograph image of a point source of light without the polarizing prism in the beam. Note the well-resolved first diffraction ring (white).

The main control computer performs all data acquisition, processing, and storage, and it controls the position of all moving elements through a remote, programmable controller that allows control of polarizing prism rotation, wavelength tuning of the blocking filter by tilting, tilting of the Fabry–Perot filter, and focusing of the CCD and associated microscope objective.

The computer also monitors the performance of the IMC; it may order offsets to track solar features that would otherwise quickly exit the field of view because of the solar rotation. Also, it remotely commands the electronic units that supply voltage to the Fabry–Perot filter and monitors that voltage and the temperature at various points through the system.

OPTICAL TESTING OF THE VECTOR MAGNETOGRAPH

The CCD system has proved to be a useful tool for testing the vector magnetograph optics, effectively replacing the need for visual inspection of the image and for specialized photometric measurements. The ability to store and manipulate single or averaged frames and to determine image profiles and statistics has proven valuable in measuring image quality and scattering in optical elements.

The system image quality was examined by imaging the diffraction pattern produced by a 10-μm pinhole onto the CCD. Figure 10 shows the image produced without any polarizing elements in place. Careful analysis of the image shows that scattering contributes to the background with a maximum value of a few percent of the peak value. The large-angle scatter (shown in green) is at the 0.1% level.

To obtain an image of such quality in a system with many surfaces, the components must have sufficient surface accuracy to produce a net wavefront distortion of less than $\lambda/4$. In general, that accuracy can be obtained with stock items from the major optical suppliers, but several lenses had to be made to order. One lens was originally obtained from low-quality stock; the result is shown in Fig. 11.

These experiments have also indicated that image quality is quite sensitive to the attitude of the lens elements to the beam, especially the final focusing lens. Best images demand that the final focusing lens be within $\pm 1°$ of the normal to the beam.

The main source of optical aberration in the system is the 25-mm-thick Glan–Laser polarizing prism. The prism introduces 1′ 50″ of beam deviation and some nonuniformity (probably due to astigmatism) in the first diffraction ring. Both effects are apparent in Fig. 12, which was generated by making multiple exposures while the prism was rotated 360°. The beam deviation was subsequently reduced to near zero without degrading the image, by judicious positioning of the other elements that rotate with the prism (dichroic polarizer, waveplate, and wedge prisms).

Figure 11—Blurred image of the point source caused by substitution of a common lens for the custom-made lens now in the vector magnetograph.

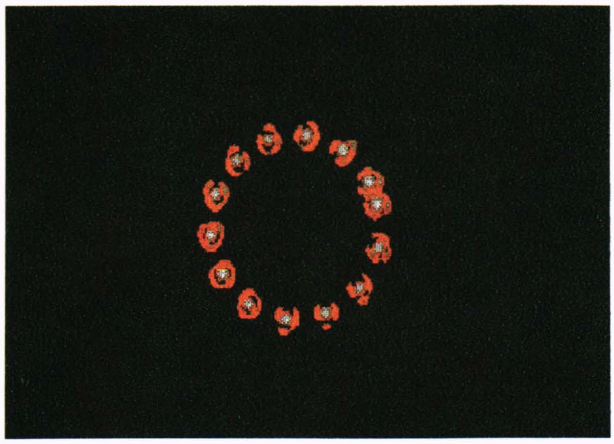

Figure 12—Effect of prism rotation on the image of a point source of light. Note the astigmatism, shown by the nonuniformity of the diffraction ring.

The image quality produced by the telescope has also been examined using the CCD camera and an autocollimating test setup. The telescope is found to be not quite diffraction-limited, probably because of significant longitudinal spherical aberration discovered in other tests. The central peak is found to be up to 20% broader than predicted by diffraction theory.

In operation, the limits on image quality will be governed by "seeing" effects cause by atmospheric turbulence. Only under the very best seeing conditions will the resolution of the system be defined by the telescope and optics. Normally, the atmosphere will blur the resolution to 1″ or 2″. The choice of Sacramento Peak Observatory for installation of the magnetograph is an attempt to maximize the periods of good seeing, but ultimately, magnetograms must be made from a spacecraft or a high-altitude balloon if the smallest and fundamentally most important features of the solar magnetic fields are to be observed.

REFERENCES

[1] Z. Svestka, *Solar Flares*, Reidel, Dordrecht (1976).
[2] R. Howard and J. O. Stenflo, "On the Filamentary Nature of Solar Magnetic Fields," *Sol. Phys.* **22**, 402 (1972).
[3] J. Heyvaerts, E. R. Priest, and D. M. Rust, " An Emerging Flux Model for the Solar Flare Phenomenon," *Astrophys. J.* **216**, 123 (1977).
[4] K. R. Krall, J. B. Smith, Jr., M. J. Hagyard, E. A. West, and N. P. Cummings, "Vector Magnetic Field Evolution, Energy Storage, and Associated Photospheric Velocity Shear within a Flare-Productive Active Region," *Sol. Phys.* **79**, 59 (1982).
[5] R. J. Bray and R. E. Loughhead, *Sunspots*, Wiley, New York, p. 10 (1964).
[6] W. A. Shurcliff, *Polarized Light*, Harvard Univ. Press, Cambridge (1962).
[7] J. O. Stenflo, "Measurements of Magnetic Fields and the Analysis of Stokes Profiles," *Sol. Phys.* **100**, 189 (1985).
[8] D. M. Rust, R. Kunski, and R. F. Cohn, "Development of Ultrastable Filters and Lasers for Solar Seismology," *Johns Hopkins APL Tech. Dig.* **7**, 209–216 (1986).
[9] M. J. Hagyard, G. A. Gary, and E. A. West, *The SAMEX Vector Magnetograph—A Design Study for a Space-Based Solar Vector Magnetograph*, 88-117, NASA Marshall Space Science Laboratory (1988).

ACKNOWLEDGMENTS—The following individuals and organizations are gratefully acknowledged for their valuable help. Kim Strohbehn and Patricia Murphy of APL designed and implemented the correlation tracker. John Townsend and Benjamin Ballard are developing the computer programs to handle solar data. Robert Moore and Harry Zink performed systems analyses and major component evaluation. Gary Starstrom designed part of the magnetograph housing. Solar photographs are from the Sacramento Peak Observatory (Sunspot, N. Mex.) of the National Solar Observatory and the High Altitude Observatory of the National Center for Atmospheric Research. Several of the figures are based on drawings in Ref. 9. The 25-cm evacuated telescope was furnished by the High Altitude Observatory. The magnetograph is being constructed at APL's Center for Applied Solar Physics, which is supported by the Air Force Office of Scientific Research University Research Initiative Grant AFOSR-87-0077.

THE AUTHORS

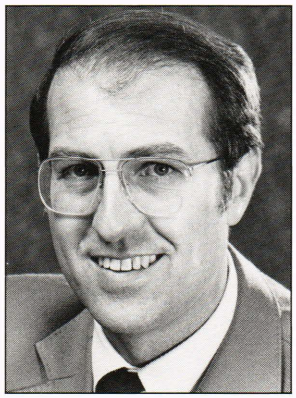

DAVID M. RUST was born in Denver, Colo., in 1939 and received a Ph.D. in astrogeophysics from the University of Colorado in 1966. Before joining APL in 1983, he was employed by American Science and Engineering, Inc., in Cambridge, Mass., and Greenbelt, Md., where he served as the Solar Maximum Mission Observatory Coordinator and as chairman of the Solar Maximum Year Study of Energy Release in Flares. Dr. Rust's specialties are in the physics of solar activity and in solar observatory instrumentation. He is a member of the Principal Professional Staff at APL and head of the Solar and Interplanetary Physics Section of the Space Physics Group. He is also director of the APL Center for Applied Solar Physics and manager of the solar magnetograph project.

TERRY J. HARRIS's biography can be found on p. 327.

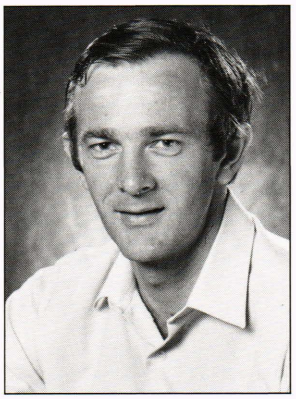

JOHN W. O'BYRNE was born in Sydney, Australia, in 1959. He received his B.S. in physics in 1981 and completed a Ph.D. in physics (astronomy) in 1986, both at the University of Sydney. His Ph.D. project involved the development of an optical interferometric system to monitor the effects of atmospheric turbulence on stellar images. As a research associate during 1986–87, he expanded this work with the development of a microthermal temperature measurement system and contributed to the optical and mechanical design of the modern stellar interferometer under construction by the Sydney astronomy group. Dr. O'Byrne is also interested in teaching astronomy and conducted astronomy courses for adults in Sydney. He came to APL in 1988 as a research associate in the Space Physics Group, joining the vector magnetograph project with responsibilities for the development, testing, and observational program of the instrument.